ELSEVIER

The 1998 Forest Fires in East Kalimantan (Indonesia): A Quantitative Evaluation Using High Resolution, Multitemporal ERS-2 SAR Images and NOAA-AVHRR Hotspot Data

Florian Siegert and Anja A. Hoffmann†‡*

Boosted by the 1997/98 El Niño-Southern Oscillation (ENSO) phenomena, uncontrolled fires have destroyed huge areas of rainforest and bush land in Indonesia. Thick smoke covered large areas over SE Asia for months. Due to their cloud and haze penetrating capability SAR sensors could complement existing fire monitoring systems based on NOAA-AVHRR data, providing a 900 times higher spatial resolution. This article describes results of the combined synergistic use of NOAA-AVHRR hotspot data received and processed by the IFFM/GTZ project and multitemporal ERS-2 SAR images for burned scar mapping in the province of East Kalimantan. Burned areas detected by ERS were verified using AVHRR sensor hot spot data and extensive field surveys during the fire season in April 1998. Furthermore, a vegetation classification discerning five classes was derived from the ERS-2 SAR images and compared to the mapped burned scars. The total burned area of the test site is estimated to be 1.3 mil ha out of 1.85 mil ha (71%). ©*Elsevier Science Inc., 2000*

INTRODUCTION

In the last two decades, fire has become one of the greatest threats to tropical rainforests, especially in Indonesia. The process of selective logging produces millions of tons of dead biomass, which serves as fuel for fires. Fire is used for large-scale land clearing, for example, for pulpwood and industrial crop plantations as well as by farmers to clear land and burn agricultural waste (Schweithelm, 1998). Because of the severe drought caused by the 1997/98 El Niño phenomena, fires could easily spread uncontrolled over large areas of rainforest, grass-, and bushland. Economists estimated the economic damage due to smoke alone in 1997 to more than 1.4 billion US$ (Schweithelm, 1998). The damage to the forest resources such as timber and plantations is uncertain due to a lack of comprehensive data. Data are also lacking for the effects on the precious and fragile ecosystem of tropical rainforest, on species diversity and soil erosion. Furthermore, biomass burning plays an important role as a major source of trace gases and aerosols in the atmosphere. This results in a strong contribution to the anticipated climate change and particularly in emissions of CO_2 fixed in the biomass as the important "greenhouse" gas (Crutzen et al., 1979; Crutzen and Andreae, 1990; Kaufmann, et al., 1990; Hao et al., 1990; Malingreau et al., 1996).

The use of remote sensing data is an efficient way to analyze the size and damage level of a burned area and following from that the ecological and economic impacts of these large scale fire events. Several approaches were undertaken to determine the extent of the 1997 forest fires in Indonesia using optical and microwave sensors. Studies were based either on the visual interpretation of multitemporal SPOT quicklook mosaics, the evaluation of NOAA (National Oceanic and Atmospheric Administration)-AVHRR (Advanced Very high Resolution Radiomoeter) and ATSR (Along Tracking Scanning Radiometer) hotspot data or the combined use of ERS-2 SAR (European Radar Satellite-2-Synthetic Aperture Radar)

* Ludwig-Maximilians University, Munich, Department of Biology, München, Germany

† Integrated Forest Fire Management Project IFFM/gtz, Kekantoran Dinas Kehutanan Tk. 1 Kaltim, Jln. Kesuma Bangsa/Harmonika, Kotak Pos 1202, Samarinda, 75001, Kalimantan Timur, Indonesia

‡ Fire Ecology Research Group, Max Planck Institute for Chemistry, Freiburg University, Freiburg, Germany

Address correspondence to F. Siegert, Ludwig-Maximilians Univ., München, Dept. of Biology, Luisenstr. 14, 80333 München, Germany. E-mail: FSiegert@zi.biologie.uni-muenchen.de

Received 27 January 1999; revised 5 August 1999.

REMOTE SENS. ENVIRON. 72:64–77 (2000)

655 Avenue of the Americas, New York, NY 10010

0034-4257/00/$–see front matter
PII S0034-4257(99)00092-9

coherence data and ATSR data (Fuller and Fulk, 1998; Wooster et al., 1998; Fang and Huang, 1998; Liew et al., 1998; Antikidis et al., 1998; Buongiorno et al., 1997).

The AVHRR sensor provides the capability to detect the presence of active fires using Channel 3 (3.8 μm). However, due to the low spatial resolution of AVHRR data images (1.1 km^2), it is difficult to exactly quantify the size of burned areas and the type of burned vegetation (Malingraeu, 1990). The evaluation of high resolution Landsat TM or SPOT images is hampered by frequent cloud cover and haze during active burning. The ERS-2 SAR sensor is able to penetrate clouds and haze and provides the high spatial resolution (25 m) necessary to identify and estimate areas. Therefore, we investigated whether multitemporal ERS-2 images could be used to survey the extent and impact of recent forest fires in Indonesia. Burned scars mapped in multitemporal ERS-2 images were verified by NOAA-AVHRR hotspots and a field study. By overlaying NOAA-AVHRR hotspots onto the ERS images, the temporal and spatial distribution of fires were investigated.

The study was conducted by the German-sponsored and GTZ (German Technical Cooperation)-implemented IFFM project (Integrated Forest Fire Management Project). The IFFM project based in Samarinda, East Kalimantan, is a technical cooperation project under bilateral agreement between the Governments of Indonesia and Germany. It is under the responsibility of the Ministry of Forestry, and implemented by the two provincial forestry agencies. Its aim is to support and build up a fire management center for the East Kalimantan province. Besides fire prevention and fire suppression activities the IFFM project provides information on fire danger, based on climate data and fire occurrences within East-Kalimantan, derived from received and processed NOAA-AVHRR data. A major aim of the study was to investigate whether multitemporal ERS-2 SAR images can complement and expand the existing NOAA-AVHRR fire detection system. Specific objectives were 1) to detect and quantify burned areas at high spatial resolution, 2) to compare AVHRR hot spots and burned scars detected by ERS-2, 3) to perform basic vegetation mapping using enhanced ERS-2 images, and 4) to produce a fire risk map for future fire prevention. Here, we focus on the results of the first three objectives.

MATERIALS AND METHODS

Study Area and Ground Verification

The IFFM project area covers the whole province of East Kalimantan (~220.000 km^2) on the island of Borneo (Figure 1). The radar project area covers 20.000 km^2 within the Kutai district. Lowland *Dipterocarp* forest and (peat) swamp forest as well as grasslands (*alang-alang*) dominate the vegetation. All forests in the project area have already been subjected to logging operations. Shifting cultivation prevails close to the rivers. Several large pulp wood and oil palm plantations have been established in the past decade. An extensive ground survey was undertaken during the fire season in April 1998. In the field we used a laptop computer in which processed and georeferenced ERS-2 images from February and March 1998 as well as NOAA-AVHRR hotspot data were stored. By connecting a Garmin 12 GPS to the laptop we were able to ascertain our actual position in the georeferenced ERS images at any given time. Most importantly, we were able to access specific areas, which we suspected as burned from SAR backscatter signals and NOAA-AVHRR hotspot data. The continuous track mode of the GPS was used to record all travel routes and in some cases burned areas. For specific sites the coordinates as well as the fire damage and the vegetation type which had been burned were noted. During the field survey more than 12 h of digital video were recorded. This material was later assigned to GPS coordinates, thus allowing identification of test sites for burned scar and vegetation signatures.

NOAA-AVHRR Data Processing and Analysis

Since April 1996, IFFM has received images from NOAA 12 and 14 satellites four times per day and since November 1998 additionally two times NOAA 15. The NOAA satellites view a broad swath of the earth from a height of about 860 km and have a spatial resolution of 1×1 km^2 (pixel size). The satellites have onboard the AVHRR (Advanced Very High Resolution Radiometer) sensor, a five-channel scanning radiometer with different spectral characteristics (visible, near-infrared, mid-infrared, and far-infrared). At IFFM the display and the quantitative analysis of the AVHRR satellite imagery is performed by Sea Scan STARS (Satellite Analysis and Research System) software. The AVHRR data is acquired by the HRPT (High Resolution Picture Transmission) Reception System, which was supplied by Sea Scan and built up by Dundee Satellite Systems (Wannamaker, 1996). The further geographical processing is done with the Geographic Analysis and Display System (GADS) and ArcView 3.1.

The AVHRR sensor has been designed for meteorological and oceanographic applications therefore special algorithms had to be developed for fire detection. The most suitable channels for fire detection are the first two "thermal" infrared channels, Channels 3 and 4. The fire detection process is based on surface temperature measurements taken by Channel 3. A pixel is detected as a fire pixel or as a hotspot when Channel 3 is saturated by a specific temperature much below that of burning vegetation (Malingreau, 1990; Kaufmann et al., 1990a, b; Kennedy et al., 1994). Therefore, to avoid false alarms detection due to high background temperature (soil), highly reflective clouds or sun reflection of water, the satellite processing program uses special algorithms. The

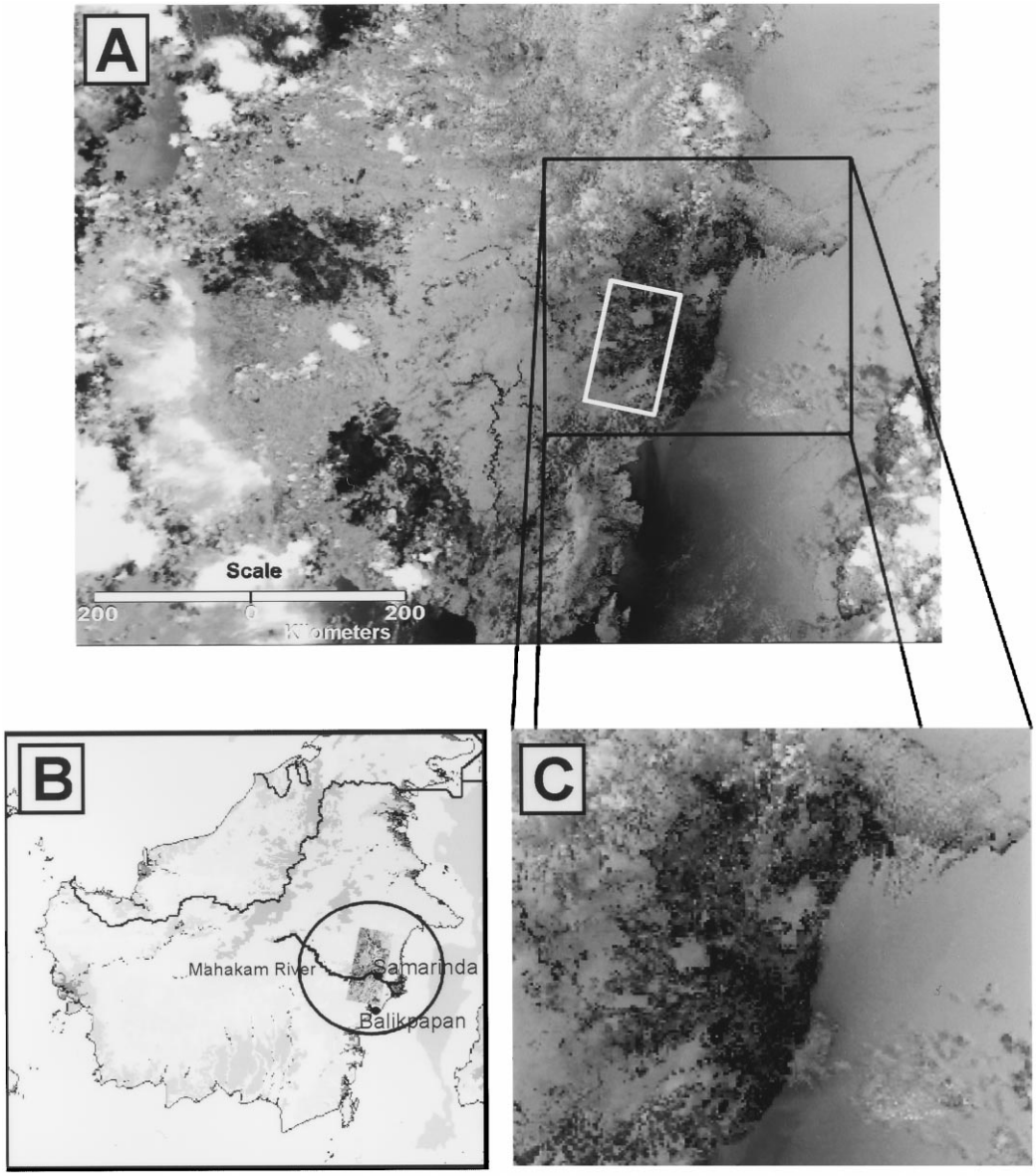

Figure 1. NOAA 14–AVHRR image of Borneo and study area: A) Channel 3 of a processed NOAA 14–AVHRR daytime image of Borneo; the white square indicates the location of the evaluated ERS scenes; B) map of Borneo; C) subset of A) as indicated. Black spots represent fire pixel or hotspots.

IFFM receiving station uses several daytime and nighttime tests. In particular, it uses the multiple threshold algorithm after Arino and Melinotte (1995) which refers to the algorithm proposed by Kaufman et al. (1990a) which updated the Dozier (1981) algorithm. The threshold temperature for Channel 3 is set manually for each image obtaining the given temperature from a screen tool. The screen tool shows the pixel distribution in relation to the measured temperature. By interactively cutting off parts of the histogram, it is possible to choose the threshold tempeature which indicates suspected fire pixels and to exclude, for example, reflection of clouds or sun glint. During the hot and dry season of January to May 1998 the threshold temperatures for daytime images ranged normally between 322° and 317°K and between 303° and 308°K for nighttime images. Provided that the surrounding background temperature is low, as during night image acquisition when a low threshold temperature can be set, the detected fire can be as small as a gas flame from an oil platform like near Balikpapan. Figures 1A and 1C show Channel 3 of a processed NOAA 14-AVHRR daytime image. Each black spot in Figure 1C represents a potential fire pixel or hotspot. Using a threshold temperature of 322°K 1273 hotspots were detected. In the course of the fire season the system did not yet provide a sea mask to mask out false detection due to sun light on the sea surface. Therefore, the processed images were rechecked and false detection eliminated.

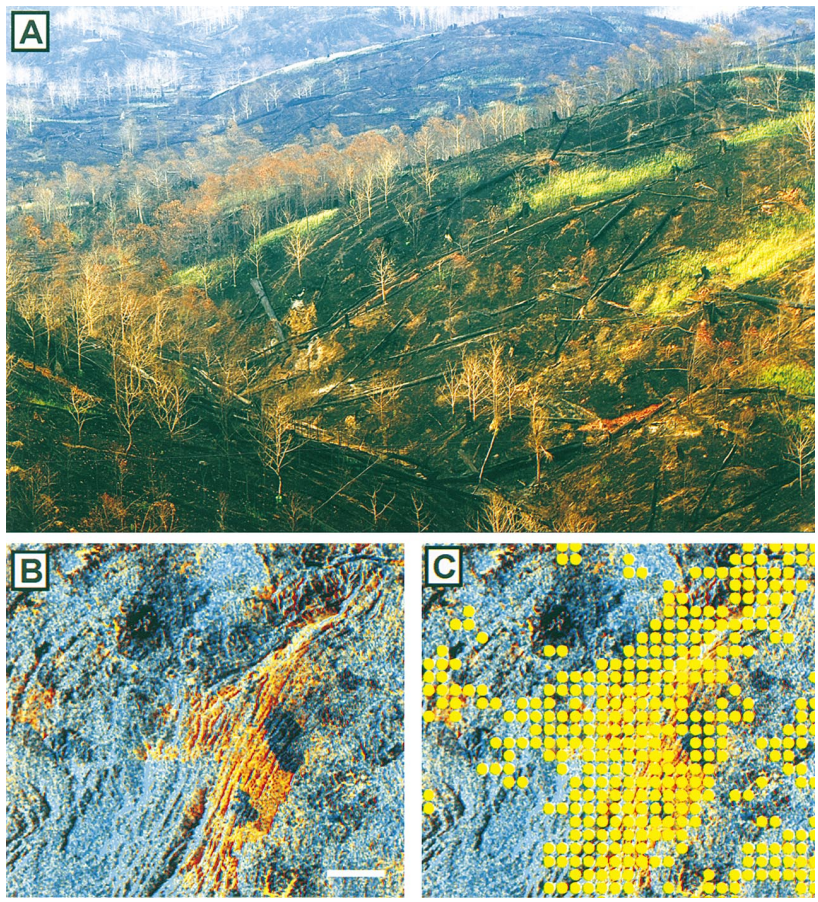

Figure 2. Comparison of a burned scar as detected by ERS and NOAA AVHRR hotspots. A) Ground photograph of the large burned scar shown in orange colors in B). This *Gmelina* sp. plantation for pulp wood was totally destroyed by fire. B) Burned scars (orange areas) as detected in a multitemporal ERS image (February–March image composite). C) The hotspots detected by NOAA-AVHRR are overlaid onto the ERS image.

A fire pixel or hotspot has a defined area of 1.1 km^2. It indicates that there is a fire or fires within this area; however, it tells nothing about the number, the size, and the intensity of the fires and the burned area (Malingreau, 1990; Dwyer et al., 1998). The hotspot coordinates represent the center of a detected fire pixel and are not real *in situ* fire coordinates. The fire or fires could be located around 500 m from the center coordinate. In general, it is difficult to precisely register a time series of approximately 200 successive NOAA-AVHRR images. The registration error depends on the operator's accuracy when overlaying the coastline to navigate the image data. Due to a coarse scale of the images (ca. 1:6,000,000) the registration quality also depends on the image quality. The more clearly visible the coastline is, the more accurate the navigation result will be. Additionally the accuracy of the AVHRR scanner deteriorates at wide viewing angles. Taken together we estimate the spatial error of the NOAA-AVHRR hotspots of up 3 km. Due to these facts a single long-lasting fire source may be represented by too many or too few hotspots in a time series of NOAA AVHRR images.

The detected hotspot coordinates have been stored in a data bank to overlay them onto the processed ERS images to verify the burned scar detection result and to show the spatial distribution of the fires. Figure 2B shows burned scars as detected in multitemporal ERS images (orange tones, see below); Figure 2C shows the hotspots as overlay onto the ERS images. As can be seen, the spatial pattern of the burned scars agrees very well; however, the area identified by hotspots is significantly larger due to the inherent error of the NOAA-AVHRR system.

ERS-2 Data Processing and Analysis

Twelve ERS-2 SAR Precision Images (PRI) acquired on six dates for two adjacent frames (3618 and 3600; Table 1) were evaluated. The location of the SAR test site is indicated by a white rectangle in Figure 1A. Here we focus on the results of the fire period from January to April 1998, which is the detection of changes between the ERS-2 Orbits 14572, 15073, and 15574. All ERS-2 SAR images except one were acquired during an extreme drought according to weather data collected from five different stations by IFFM (Table 1). Adjacent scenes were mosaicked and map-registered using a set of ground control points derived from GPS measurements and topographic maps. Visual inspection of raw, unprocessed ERS images allowed only for discrimination between geomorphologic structures and large water bodies like lakes and rivers. Even a distinction between forest/nonforest was impossible. To be able to discriminate different vegetation and land-use classes, monotemporal ERS images

Table 1. ERS Orbits, Acquisition Dates, and Weather Conditions during Image Acquisition

Orbit No.	*Acquisition Date*	*Prevailing Weather Conditions*
12067	11 Aug 97	Dry since 20 days
12568	15 Sep 97	Dry since 50 days
14572	02 Feb 98	Dry since 14 days
15073	09 Mar 98	Dry since 35 days
15574	13 Apr 98	Dry since 65 days
16075	18 May 98	Moist since 7 days

were subjected to three separate speckle and texture filtering operations. The filter products (7×7 gamma map filter for speckle reduction, 10×10 variance filter, and 20×20 variance filter) were then combined into artificial ERS RGB composite images by assigning each filter product to a different color channel (Siegert and Kuntz, 1999; Kuntz et al., 1996). A comparison of Figures 3A and 3B shows that more features can be discriminated visually in the RGB composites than in the unprocessed or simply speckle filtered ERS image.

Visual inspection of a time series of gamma map filtered ERS-2 images showed that there is a clear change in radar backscatter and/or image texture when fire has affected vegetation. Burned areas appear considerably darker in speckle-reduced images. Ground verification showed that this can be attributed to a partial or complete removal of the plant cover. Severe burns, which destroy the vegetation cover completely, result in a dramatic change towards a very low backscatter from reduced volume scattering and bare and dry soil and a decreasing dielectric constant (Figs. 4A and 4B, e.g., upper left corner). A detailed analysis of backscatter signals before and after fire impact will be published elsewhere (Siegert and Rücker, 1999; 2000). The detection of burned areas was based on the multitemporal evaluation of the changes that occurred between two ERS overpasses before and after the fires, by performing a principal component analysis (PCA). After the transformation, the first component holds information on common features in both images—geomorphology and some texture information—while the second component contains the differences between the two images and thus indicates change. Component two was then combined with two gamma map filtered ERS images (e.g., February and March) to give an RGB color-composite image for further visual interpretation. The advantage of this representation is that it displays the change and at the same time preserves the geomorphology and texture information at a high spatial resolution (Fig. 4C: red: PCA Band

Figure 3. Production of an ERS RGB image and the corresponding vegetation map. A) Gamma map filtered ERS-2 image mosaic acquired before the fires in August 1997 (11 August 1997). B) RGB composite of A) (see text) (red: 10×10 texture filter, green: 7×7 gamma map filter, blue: 20×20 texture filter). C) Result of the visual vegetation classification. Different colors indicate different vegetation types. Dark green: selectively logged *Dipterocarp* forest; bright green: undisturbed (peat) swamp forests; red: clearings with open soil and very low vegetation; light yellow: plantations and regrowing forest agriculture; brown: *alang-alang* grass and strongly degraded forest. Bar: 20 km.

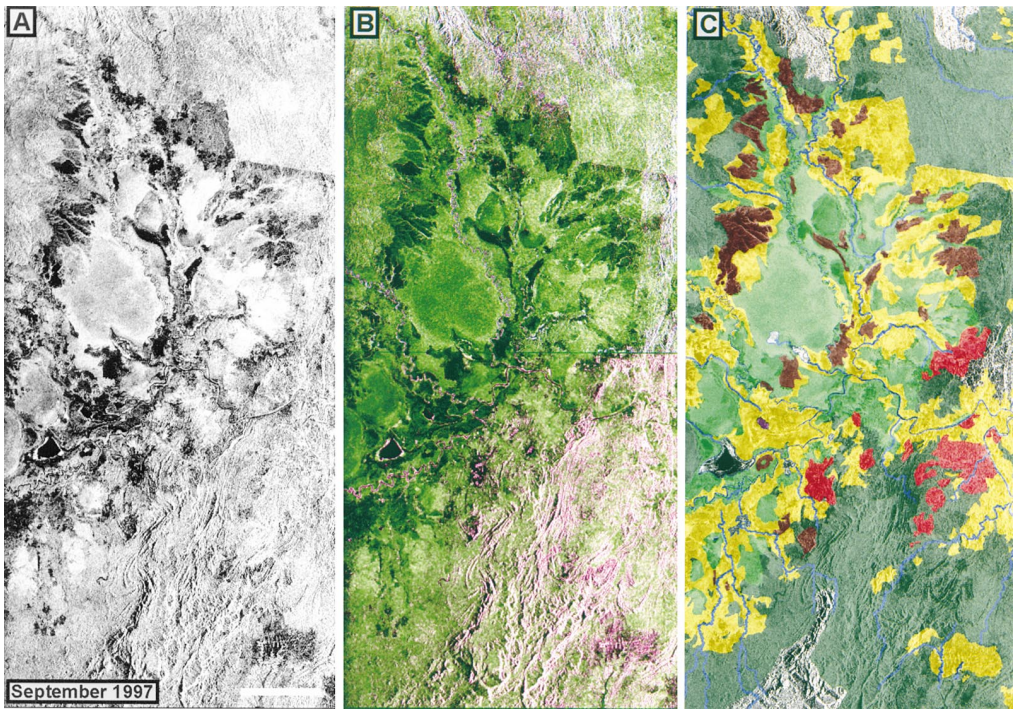

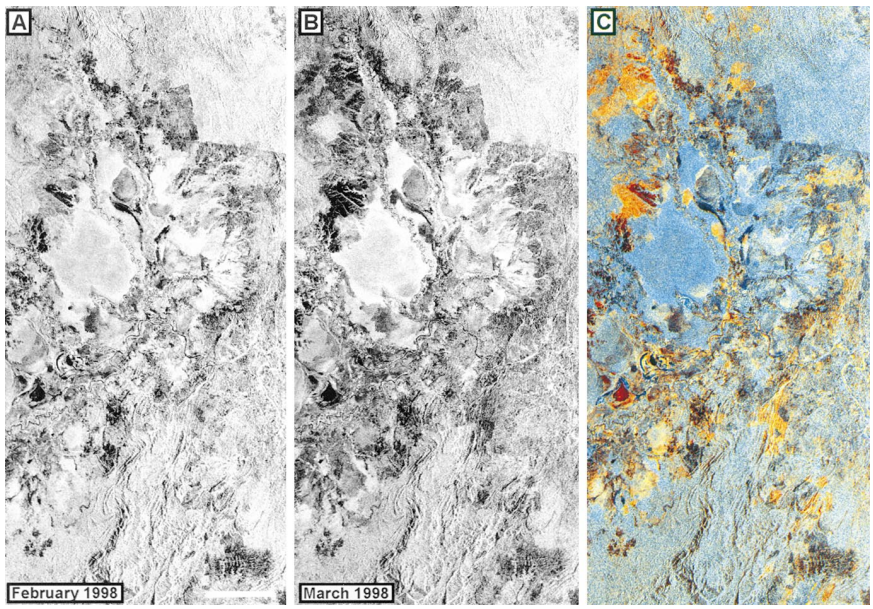

Figure 4. Production of a multitemporal ERS PCA image. Gamma map filtered ERS-2 image mosaic A) acquired in February 1998 (Orbit 14572) and B) acquired in March 1998 (Orbit 15072). C) PCA composite showing unburned vegetation in blue colors. Burned areas appear in different shades of orange depending on the severity of damage. Red: PCA Channel 2 (see text); green: February gamma map filter; blue: March gamma map. Bar: 20 km.

2 displaying changes between February and March; green: February image; blue: March image). Burned areas are visible in orange tones of different intensity; unburned vegetation appears in blue tones. Processed ERS SAR color images were visually interpreted to identify vegetation types and burned scars using the GIS software ArcView 3.0 by manually delineating areas belonging to each of the various classes.

RESULTS

NOAA-AVHRR Data Evaluation

The dry weather conditions created by the El Niño phenomena in East Kalimantan lasted until May 1998. No substantial rainfall was recorded in Samarinda and Balikpapan from January until the end of April, whereas all the other provinces in Kalimantan and Sumatra and northerly parts of East Kalimantan had experienced normal to heavy rainfalls in the beginning of March. This is also visible in Figure 1 (AVHRR image from 5 March 1998) by swollen rivers in Central Kalimantan (e.g., Barito River). Such clear and cloud-free images were received only during the El Niño phenomena and are not usual for tropical regions. In mid-January NOAA-AVHRR detected hotspot numbers began to rise correlating with the fire danger index [a metric index based on rainfall and temperature data derived from the Keetch–Byram Drought Index after Deeming (1995) for the IFFM project]. Figure 5 shows the relationship between all detected NOAA 14 daytime hotspots (period January-May), the cloud coverage taken by a simple threshold test in Channel 2 during calculating the NDVI (normalized difference vegetation index) and the drought index. Due to the fact that the NOAA-AVHRR receiving station was not running all the time, the hotspot graph is not continuous. The actual receiving time is shown in gray columns, meanwhile the off-time is indicated by white. Additionally, the detection is also depending on cloud coverage, since the AVHRR sensor is not able to penetrate clouds. Therefore, low hotspot numbers generally correspond to higher cloud coverage. The cloud coverage in Figure 5 is given for the whole processed image as represented by the NOAA-AVHRR image in Figure 1 and not only for the fire area. In spite of that, there is a clear correlation between the rising drought index and numbers of detected hotspots. At the end of February the detected hotspots rose up to 600 and peaked at the beginning of March with more than 2000 hotspots per day meanwhile the drought index had almost achieved its maximum value (2000). Figure 6 shows the temporal evolution and the spatial distribution of the detected hotspots within the study area. By the time the rain started at the beginning of May almost all of the basin area in the district of Kutai had been burned. The fire affected the whole of the Mahakam basin, its tributaries and as can be seen in Figure 7 reached up as far as the Sangkulirang peninsula. In Figure 7 yellow, indicates hotspots detected in February; red, hotspots detected in March; and purple, hotspots detected in April. The fires started at the center of the basin and propagated south, only stopping in the mountainous regions to the west and north where humidity is much higher and primary forests dominate and logging operation has not yet progressed that far.

ERS SAR Evaluation

Vegetation and Land Use Mapping

To be able to estimate the economic damage to the forest resources such as timber and plantations and ecological impacts on this fragile ecosystem caused by the fires, as well as to roughly calculate the CO_2 emissions, it is

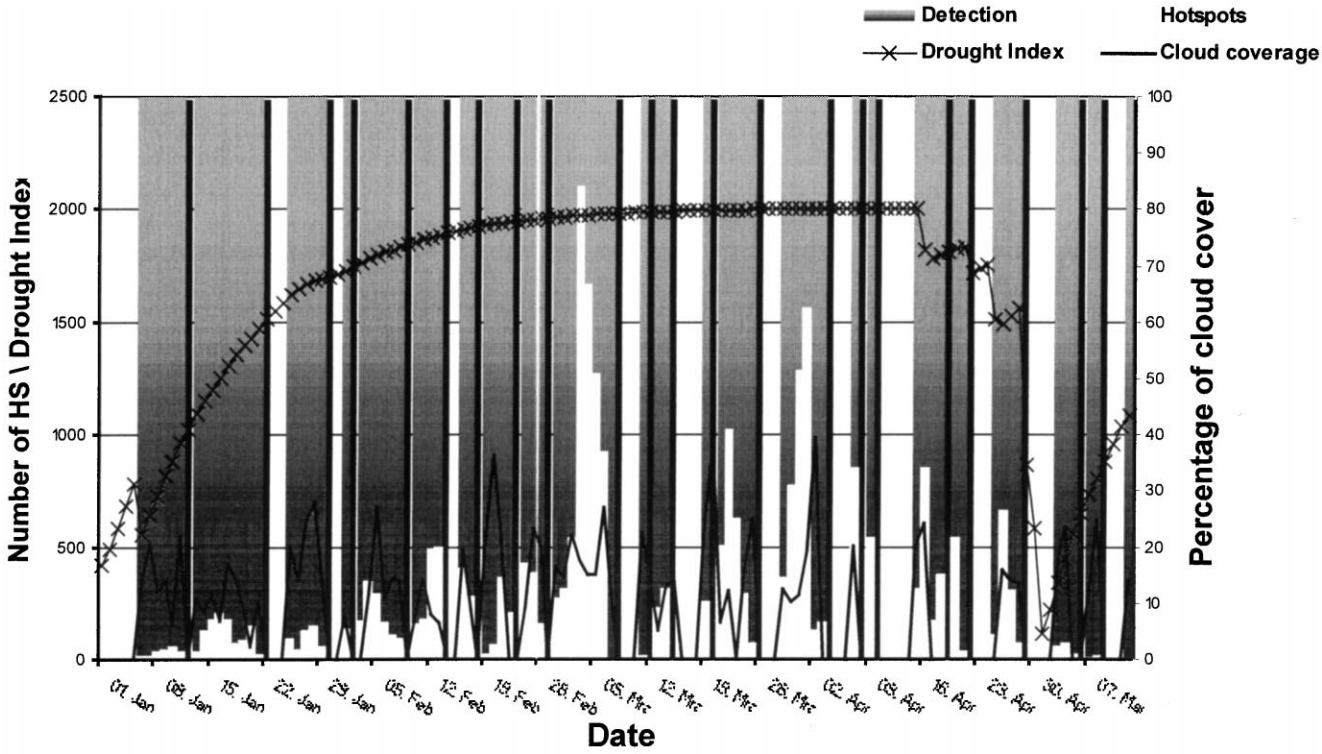

Figure 5. All detected NOAA-AVHRR 14 daytime hotspots (period January–May) (white bars), cloud coverage (solid line), and drought index. The time of AVHRR acquisition is shown in gray columns; the off-time is indicated by white.

necessary to map the burned scars with high spatial resolution and intersect this data with a vegetation map. However, a recent reliable vegetation map was not available for this region of Indonesia. The most recent data available to us was a map provided by INTAG (Mapping and Inventory Unit of the Ministry of Forestry) which represented the status of 1992 based on Landsat TM images of the late 1980s. From field surveys we knew that this information is not up-to-date for most of the radar test site. A vegetation map derived from NOAA-AVHRR images was too crude for our purpose (Achard and Estreguil, 1995). Recent, cloud-free Landsat TM or SPOT images were not available for the complete test site. Therefore, we used monotemporal ERS images acquired shortly before the fires (11 August 1997) to produce a simple, but up-to-date, vegetation and land use map. In flat terrain, monotemporal RGB color composites allow for discrimination of several different vegetation and land use classes based on the structure of the canopy and water content of the leaves (Siegert and Kuntz, 1999). With the knowledge acquired during three field surveys (1995, 1996, 1998) a classification key for

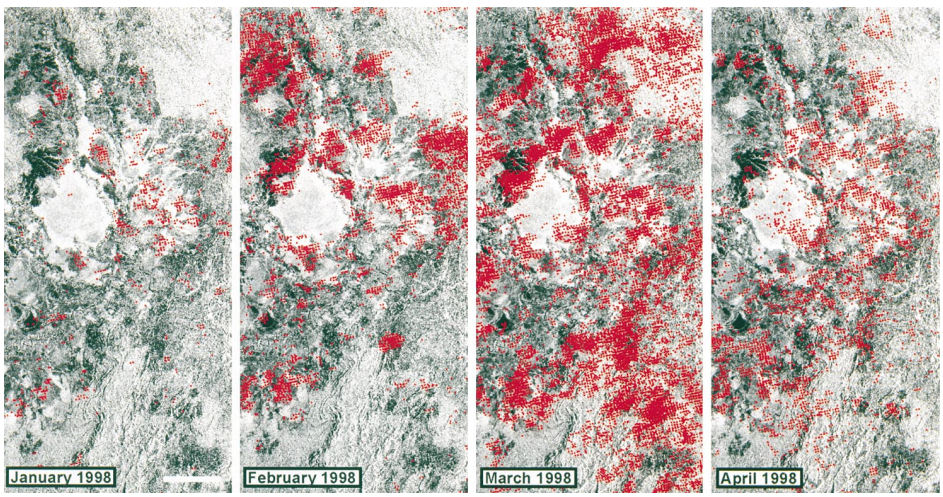

Figure 6. Spatial pattern of detected hotspots within the ERS study area from January (A) to April (D) 1998. The hotspots are overlaid onto an ERS image acquired before the fires in August 1997. According to these data almost all of the basin area in the ERS study area has been burned. Bar: 20 km.

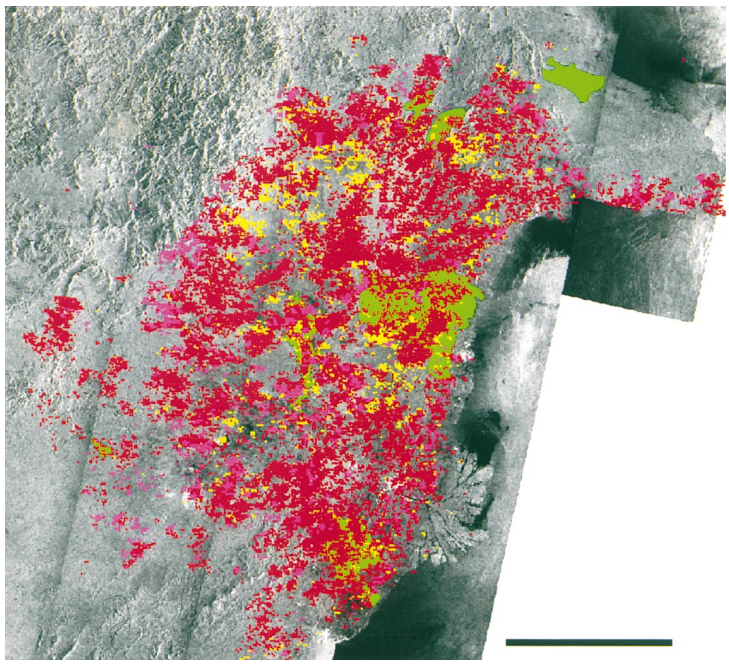

Figure 7. ERS quicklook mosaic and NOAA-AVHRR hot spots showing the area (400×400 km) affected by fire. The ERS mosaic was made from quicklooks downloaded from CRISP (Singapore). The fire devastated the whole Mahakam basin and went up its tributaries as far up as to Sankulirang peninsula. Yellow indicates hotspots detected in February; red, hotspots detected in March; and purple, hotspots detected in April. Green areas indicate protected forests as Kutai National Park. Bar: 100 km.

the interpretation of the ERS RGB images was established which made it possible to discern five different vegetation classes relevant to the questions raised above (Fig. 3C):

1. Selectively logged *Dipterocarp* forest. In these forests the closed canopy has been opened up to a variant degree. On lone-standing trees corner reflection occurs and volume scattering is increased. Occasionally the radar signal can reach the ground and bare soil contributes to the backscatter signal. This class shows a mosaic-like pattern of green and magenta-white spots in the RGB image, for example, Kutai National Park (rectangular shape) in the upper right corner of Figure 3B. There are no primary (undisturbed) *Dipterocarp* forests in the project area, which would have a different signature.
2. (Peat) Swamp forest. A relatively smooth canopy showing reduced volume scattering characterizes this forest type. This vegetation type appears homogeneously green in the RGB composites, for example, the oval shape slightly left of the center in Figure 3B. This class may be confused with pulp wood plantations over 4 years old.
3. Clearings with sparsely covered soil, for example, coal mining, appear as a speckled white-magenta pattern, if the backscatter is dominated by relief features. Small-scale relief features are usually not visible since they are leveled out by the forest canopy.
4. Plantation areas, fallow areas, bushland, and degraded forests are characterized by different stages of low growing vegetation. In RGB images from the dry season these areas appear as a heterogeneous pattern of light and dark green colors, roughly corresponding to the height/biomass of the vegetation, for example, below and to the left of Kutai National Park in Figure 3B.
5. *Alang-Alang*, ferns, and low bushes: This vegetation class grows predominantly in areas frequently affected by fire and on degraded or siliceous soils, which dry out quickly. It has very low backscatter values on all channels due to backscatter from dry soil and a smooth, homogeneous appearance of the plant cover, visible, for example, in Figure 3B to the left of the oval shaped swamp forest. In single RGB composites this class cannot be discriminated from land clearing operations, for example, for plantations in flat terrain. However, land-clearing operations can be distinguished in multitemporal series.

Figure 3C shows the results of the vegetation classification. During the visual interpretation available field data was included. The ERS based classification was then digitally compared to a vegetation classification by INTAG 1992 (Forest Mapping and Inventory Unit of the Ministry of Forestry) available as GIS layer and updated using concession maps and digital GIS information on plantations and timber concessions (*Dipterocarp* forest). In Figure 3C the georeferenced GIS interpretation was placed on top of the gamma-map filtered ERS image. Mountainous regions unsuitable for image interpretation were masked out. Dark green represents selectively logged *Dipterocarp* forest and bright green as then undisturbed (peat) swamp forests. Clearings with open soil and relief features appear in red. The complex pattern

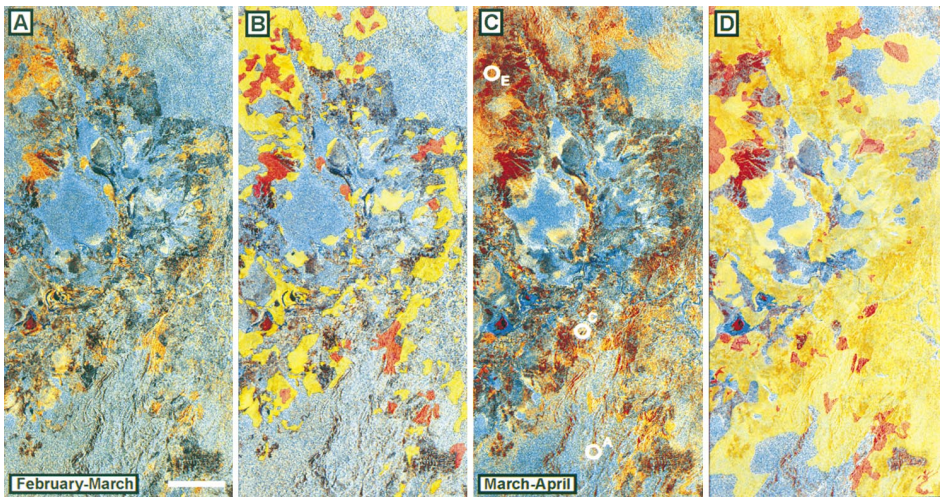

Figure 8. Mapping of burned scars in multitemporal ERS PCA images. A) February–March composite. In A) and C) orange colors indicate burned areas; blue colors unburned vegetation. B) GIS overlay of the visual classification of burned scars. Red depicts complete burn of the vegetation; yellow severe damage but incomplete burn. C) March–April composite and D) GIS overlay. Circles in C) indicate the radar signature of different damages to the vegetation as shown in Figure 9. Bar: 20 km.

of fields, fallows, plantations, and regrowing forest is colored light yellow. Brown designates *Alang-Alang* grassland, ferns, and shrubs.

Detection of Burned Vegetation

Figures 8A and C show burned scars in multitemporal ERS composites, which occurred between February and March (A) and March and April (C) ERS-orbits. Burned scars are visible as orange colors of different intensities, unburned vegetation appears as blue colors. A comparison with all hot spots detected in the area during this period showed agreement between both data sets (compare Figs. 8 and 6). Using field data of known burned scars, the GPS tracks in conjunction with digital video and hotspot data, a classification key for the interpretation of the multitemporal ERS composites was established. This made it possible to discern two different classes of fire damage: 1) severe damage, that is, total destruction of the vegetation by the fire (Figs. 9D and F), and 2) medium damage, that is, up to 50% of the vegetation cover having been burned (Fig. 9B). Both damage classes were closely related to the vegetation types affected by the fires. For example, severe damage was found predominantly in degraded forests and grasslands (*Alang Alang*, etc.) while medium damage was found predominantly in *Dipterocarp* forests. Intense orange colors corresponded to severe damage, while medium damage can be readily detected in multitemporal ERS-2 images as having a specklelike appearance: intense orange pixels (indicating a strong decrease in image brightness) are interlaced with blue-green pixels (indicating little change between the two images), for example, as visible in the lower part of Figure 8A. Different degrees of vegetation damage can also be seen in Kutai National Park in Figure 8C (square shaped feature in upper right), ranging from total destruction (intense orange) to medium damage (few yellow pixels interspersed with homogeneous blue). It was not possible to classify these two signatures using supervised classification algorithms. Therefore, we classified the PCA composites visually to produce burned scar maps as shown in Figures 8B and 8D. Yellow coloring of the delineated polygons indicates a medium damage to the vegetation and incomplete burn, while red indicates an almost complete burn of the vegetation cover.

By analyzing successive PCA composites, it became possible to monitor the fire propagation and expansion of the burned scars. In Figure 8C areas appear in dark brown if they had burned between February and March while areas which had burned in the period March to April appear in orange colors as in Figure 1A. This was confirmed by NOAA-AVHRR hotspots data. There was a tremendous increase in the burned surface area between February and April. In the February–March image fires occurred mainly in areas with degraded forest or plantations. Meanwhile the relatively well preserved rain forests of Kutai National Park (upper right in Fig. 8A) and a timber concession (the mountainous region in the lower part of Fig. 8A) remained almost unaffected. By April, fire had destroyed large parts of National Park and the timber concession (Fig. 8C).

The total area investigated by the ERS SAR study was 1,860,000 ha. Out of this up to the 9 March (February–March composite) 462,000 ha (23%) had burned (85,000 ha complete destruction of the vegetation). By 13 April 1,230,600 ha (66%) had burned, with 101,920 ha (5.5%) being completely destroyed, that is, all together 71.5% of the total area was severely affected by fire. A comparison of the GIS layers of vegetation classification (Fig. 3C) and the results of the multitemporal ERS image evaluation (Figs. 8B and 8D) allowed for the type of vegetation destroyed by the fires to be determined. Table 2 shows quantitative results of this analysis. As can be seen, the fires affected predominantly degraded forests and logged forests. Mountainous areas covered with yet undisturbed or less intensely logged

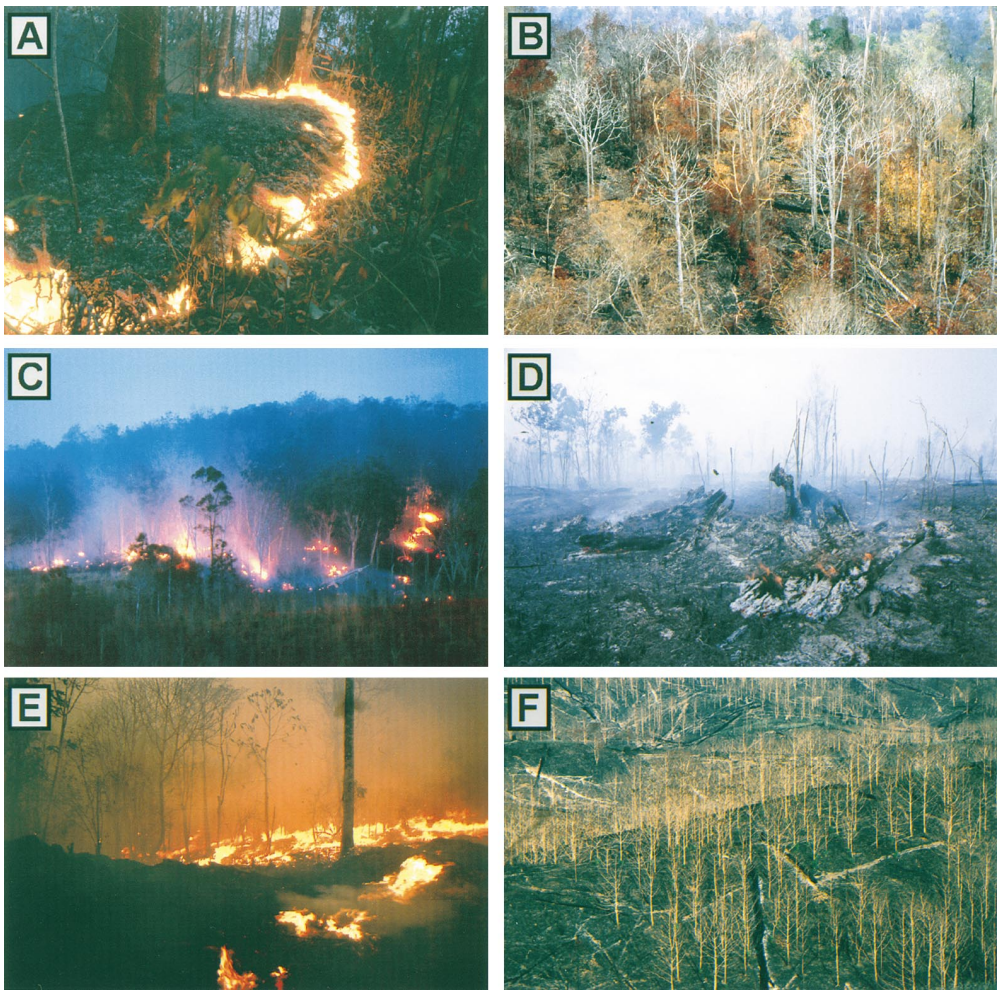

Figure 9. Different types of fires and the damage they cause: A) weak ground fire in a selectively logged forest; B) medium damaged logged over forest; C) intensive fire in a logged forest; D) complete destruction of a selectively logged forest; E) intensive fire in a pulp wood plantation; F) completely destroyed pulp wood plantation.

Dipterocarp forest and peat swamp forests were less affected by fire than already degraded vegetation types such as, for example, *alang-alang* grasslands.

DISCUSSION

In 1982/1983 during the ENSO-related drought, Indonesia was hit by severe fires affecting approximately 5 million hectares (ha) of primary and secondary forests as well as other land-use systems on Borneo (Malingreau et al., 1985). In the Indonesian province of East Kalimantan alone more than 3.2 million ha were burned (Schindele et al., 1989). Again in 1997/1998 Indonesia experienced perhaps the greatest fire disaster of its own and global history. Alone in East Kalimantan the areas affected were 5.2 million ha (paper in preparation). In order to be prepared to prevent such disasters in the future, the causes and the consequences of the recent forest fires have to be analyzed carefully. Due to the large area affected by fire and the inaccessibility of the region, the analysis has to rely on spaceborne remote sensing data. However, within 1 year after the fires, it was not possible to acquire a sufficiently cloud-free mosaic from the fire affected area in East Kalimantan by optical satellites. Cloud-free Landsat TM, IRS, or SPOT images would be ideal for burned scar mapping; however, over the course of time it becomes increasingly difficult to reliably map burned scars from optical images due to the fast regrowth of underbrush and vines. Antikidis et al. (1998) used radar coherence images derived from an ERS tandem mission to discriminate forest/nonforest and in conjunction with ATSR-derived hotspot data to map burned scars in Kalimantan. This method proved to be very useful; however, it has the major drawback that ERS tandem data are not available regularly. Therefore, we investigated whether standard ERS images as they are acquired every month throughout the year can be used for burned scar mapping in a multitem-

Table 2. The Area Affected by Fire, Damage Intensity, and Vegetation Types inside the Study Area

	Total Area Size in Hectares	*Mountains, Generally* Dipterocarp *Forest*	*Selectively Logged* Dipterocarp *Forest*	*(Peat) Swamp Forest*	*Plantation, Bush and Degraded Forest*	Alang-Alang, *Ferns, Shrubs*
Total area in ha and %	1.865.000	112.800	742.600	344.500	518.500	146.900
	100%	6%	40%	18%	27.5%	8.5%
Severe damage in ha and %	101.920	164	63.700	9.700	24.000	4.400
	5.5%	0.01%	3.4%	1%	1.2%	0.3%
Medium damage in ha and %	1.230.600	62.070	511.800	180.400	374.800	101.600
	66%	3.3%	27%	10%	20%	5.7%
Unburned or slightly burned in ha and %	532.590	50.600	167.000	154.400	119.700	40.900
	28.5%	2.6%	9.4%	7.3%	6.3%	2.5%
Burned area of each class in %	—	55%	77.5%	55%	76.9%	72%

poral approach. The analysis of multitemporal time series of processed ERS-2 images acquired before, during, and after the fire season allowed for the detection of burned scars at high spatial resolution, due to a significant reduction in the backscatter signal after burning, no matter what kind of vegetation was affected. Prevailing vegetation types in the project area are mainly logged forest, undisturbed (peat) swamp forest, plantations, shrubs, and grassland. With the use of the GPS and the georeferenced ERS-2 images, it was possible to access specific areas which showed a striking decrease in backscatter in successive ERS SAR images in the field. Field data suggested that the observed decrease in backscatter was caused by fire. The weaker backscatter signal upon fire damage is most likely caused by a decrease in volume scattering from the opened canopy and a reduced leaf biomass. Furthermore, if the canopy was damaged to a varying degree by the fire, backscatter from soil will contribute more significantly to the signal detected by the SAR sensor. Since a soil's radar reflectively depends on its moisture content, dry soil appears dark in radar images while moist soil has a bright signature (Ulaby et al., 1986). In boreal forests it was found that ERS backscatter strongly increased in fire scars due to an increase in soil moisture content (French et al., 1996).

The amount of damage fire will cause to vegetation depends on many different parameters such as available fuel, the type and water content of vegetation, amount and type of dead biomass, wind, etc. As a result, local damage to the vegetation varies to a large extent. We found that at least two categories of burning can be identified in the processed ERS images—a complete burning of the vegetation (severe damage) and a thinned out canopy (medium damage). Undergrowth burning cannot be recognized in ERS images if the canopy of the forest remains intact. Figure 9 illustrates the different types of burn intensity and the damage they cause. All photographs were acquired during the field excursion of April 1998 and can be located in the ERS image (see circles in Fig. 8C). Figure 9A shows a ground fire of weak intensity in a selectively logged forest. Such fires propagate along the forest floor and cause varying amounts of damage to the trees, depending on the density and desiccation of the understory vegetation. There is a clear correlation between the damage caused by fire and the prior intensity of logging operations. (Schindele et al., 1989). If logging had only low impact, then the fire produced little thermal energy, and the damage to the trees was correspondingly low. If the canopy was heavily disturbed, a dense understory vegetation of fast growing pioneer species could develop, which gave an ideal fuel load for fire. Huge amounts of highly combustible logging waste also increased the fuel load. Once ignited, tree stumps may glow for days and are a constant source of fire. Figure 9B shows a severely damaged selectively logged forest in the Bukit Soeharto Recreation Forest. Some larger trees survived the fire, but most of them have lost their foliage completely and died due to bark damage. Such areas are highly in danger of being starting points for future fires. Figure 9C shows a severe fire in a strongly degraded logged forest; Figure 9D shows the remains after such a severe fire. Plantations were especially prone to fire. In poorly managed 5–10-year-old *Albicia* or *Gmelina* plantations, we found a completely desiccated, highly combustible dense understory of vegetation which gave rise to the most intense fires with complete destruction of the vegetation (Fig. 9E and 9F). It must be considered that the change detection method used here to detect burned scars might identify land clearing operation, for example, for agriculture or industrial crops as fire damage and thus cause an overestimation of the burned area. In east Kalimantan as well as in whole Indonesia almost all land clearing for plantations is done using fire; furthermore, agriculture is almost entirely based on shifting cultivation (Schweithelm, 1998). Agricultural activities were minimal due to the severe drought caused by the 1997/1998 El Niño-Southern Oscillation (ENSO) event any crop growth was greatly reduced. Furthermore, possible misinterpretations, although unlikely, could be avoided by checking for AVHRR hot spots.

Among the actual available remote sensing systems

the NOAA-AVHRR system has proved to be very efficient for the detection and monitoring of vegetation fires (Gregoire, 1996). Moreover, the NOAA-AHVRR system plays an important role as a data source in the development of a "Global Fire Product for Global Change Studies" (Malingreau and Grégoire, 1996). Within the Integrated Forest Fire Management Project the NOAA-AVHRR fire monitoring system is used to provide information on fire occurrences mainly in East Kalimantan. Since the IFFM/GTZ project receives AVHRR data in real time and, due to the high temporal resolution, a maximum six times a day, the NOAA-AVHRR system guarantees almost continuous monitoring, and therefore it could lead to taking immediate action to suppress the fires or prevent further damage. During the escalating fire season of 1998 (January to mid-May) in East Kalimantan IFFM delivered the daily hotspot data by facsimile and official letter to several government institutions. Few government institutions attempted to use the hotspot data to monitor the forest fires and to undertake fire suppression actions (Hoffmann and Christy, 1998). Nevertheless, the AVHRR detection results are hampered by clouds and haze. Furthermore, to access the precise fire location seems to be difficult because of the low spatial resolution of the AVHRR sensor and additionally due to the uncertain image registration. The coordinates might have an error of approximately 3 km, and care should be taken when using the data for applications where precise location is needed (Grégoire et al., 1996). Several approaches have been undertaken to discriminate burned areas from nonburned areas in boreal (French et al., 1995; Cahoon et al., 1994) and tropical areas (Frederikson et al., 1990; Fuller and Fulk, 1998) either by using of the minimum value composite of Channel 2 of AVHRR data or mostly using the AVHRR NDVI. However, for assessing burned scars precisely using these methods, the ability of the NOAA-AVHRR system is limited (Heriosa et al., 1995). An algorithm for extracting burned areas from a time series of AVHRR GAC data applied at a continental scale was developed by Barbosa et al. (in press). We found that burned scar mapping with high resolution imagery as ERS-SAR data can be verified by NOAA-AVHRR data. Additionally NOAA-AVHRR data can assist in determining areas of interest prior to the acquisition and processing of high resolution imagery (Grégoire, 1996). NOAA-AVHRR data provides, in addition to actual hotspot data, seasonal patterns of vegetation development (fuel conditions) derived from NDVI data. When implemented in a computer-based fire information system and further combined with other sources of information such as additional land use information (e.g., forest planning), settlements, climate data, and topographic data, as well as other relevant information of human activity it provides means for the prediction of fire-prone areas and thus supports to the essential goals of the IFFM project, these being fire management planning, prevention, and suppression.

Our work shows that multitemporal ERS-2 SAR images can complement existing AVHRR sensor fire monitoring systems in four important ways: 1) During active burning fires, burned scars can be located with high accuracy. In conjunction with daily NOAA-AVHRR hotspot data burned scar mapping can be verified. Furthermore, the analysis of hotspots supports planning for immediate action to prevent the spreading of the fires. 2) Different intensities of damage can be identified, thus improving estimates of economic and ecological impacts. 3) Derived from burn intensities, the remaining fuel after the burning could be estimated, hence providing valuable information for the prevention of future fires in the same area. 4) Digitally enhanced ERS-2 images allow for basic vegetation mapping. In conjunction with the exact location and extent of burned scars, they provide important data on biomass burning and its contribution to global warming.

Operational usage of SAR data for fire monitoring and burned scar detection in the future will need a continuous supply of data. Right now there are several space borne SAR systems available, which operate at different frequencies, polarization, and incidence angles: the European ERS-1 and ERS-2 satellites use C-band and VV polarization with an exact repeat of orbit of 35 days, the Japanese JERS satellite uses L-band and HH polarization with an exact repeat orbit of 48 days, and the Canadian RADARSAT with C-band and HH polarization, variable look angles (20–50°) and a higher spatial resolution. Successors are planned for the ERS satellites (ENVISAT), JERS (JERS-2), and RADARSAT (RADARSAT-2) within the next 2–4 years. Unfortunately, JERS stopped operation in October 1998, although preliminary results indicated that the L-band could also be useful for burned scar mapping in tropical regions (in preparation; Rignot et al., 1997). ERS-1 was launched in 1991 and is still operational. It is planned by ESA to continue to operate ERS-1 and ERS-2 till the end of the commissioning phase of ENVISAT (by the year 2001). Since the ASAR instrument onboard ENVISAT will also operate at C-band and VV (and HH) polarization, there will be continuity in data supply between ERS and ENVISAT. If ERS-1 and 2 are still working at that time, there will also be the opportunity to decrease the orbit repeat time, thus allowing for a more detailed analysis of the origin and spreading of fires during active burning.

Outlook

In order to obtain more detailed information on the total area affected by fire in East Kalimantan, an extended ERS-2 SAR-NOAA-AVHRR project was begun in December 1998. This project covers all the flat areas in East Kalimantan with ERS-2-SAR images (46 ERS

scenes, approximately 20,000,000 ha land area) acquired before and after the fires. The results will be used by the two ongoing GTZ forest projects in East Kalimantan, Integrated Forest Fire Management (IFFM) and Promotion of Sustainable Forest Management Project (SFMP), which are both financially supporting this large scale ERS-SAR investigation. The main purpose of this investigation is to propose and support a step-by-step action plan to the Indonesian forest sector. The remote sensing data will be the first step to assess in an objective way the extent of damage from the 1997/1998 forest fires. Since the stocking volume of the fire affected production forest has been decreased substantially in many areas, it is necessary to revise plans for annual cutting amounts for sustainable forest management and to establish plans for rehabilitation. Furthermore, more precise figures on economic and ecological damage, estimates of CO_2 emissions and information on future fire risk will be available for the whole province.

We wish to thank IFFM/GTZ for financial support, L. Schindler, the IFFM team leader in Samarinda, for his support of the project as well as the complete IFFM project staff. We also thank Gernot Rücker; who did a lot of SAR image processing and GIS work, and further Brian Wannamaker (Sea Scan, Canada) for his support of the NOAA-AVHRR receiving station.

REFERENCES

Achard, F., and Estreguil, C. (1995), Forest classification of Southeast Asia using NOAA AVHRR data. *Remote Sens. Environ.* 54:198–208.

Antikidis, E., Arino, O., Laur, H., and Arnaud, A. (1998), ERS SAR coherence and ATSR hot spots: a Synergy for Mapping Deforested Areas. The Special Case of the 1997 Fire Event in Indonesia. In *Proceedings of the Retrieval of Bio- and Geo-Physical Parameters from SAR Data for Land Applications Workshop ESTEC*, 21–23 October, Netherlands, ESA SP 441.

Arino, O., and Melinotte, J. M. (1995), Fire index atlas. *Earth Obs. Quart. ESA* 50:11–16.

Barbosa, P. M., Grégoire, J.-M., and Pereira, J. M. C. (1999), An algorithm for extracting burned areas from time series of AVHRR GAC data applied at a continental scale. *Remote Sens. Environ.* in press.

Buongiorno, A., Arino, O., Zehner, C., Colagrande, P., and Gorly, P. (1997), ERS-2 monitors exceptional fire event in South-East Asia. *Earth Obs. Quart.* 56–57:1–6.

Cahoon, D. R., Stocks, B. J., Levine, J. S., Cofer, W. R., III, and Pierson, J. M. (1994), Satellite analysis of the severe 1987 forest fires in northern China and Southeastern Siberia. *J. Geophys. Res.* 99(9D):18,672–18,638.

Crutzen, P. J., and Andreae, M. O. (1990), Biomass burning in the tropics: impact on atmospheric chemistry and biogeochemical cycles. *Science* 250:1669–1677.

Crutzen, P. J., Heidt, E. L., Krasenec, J. P., Pollock, W. H., and Seiler, W. (1979), Biomass burning as a source of atmospheric gases CO, H_2N_2O, CH_3CL, and COS. *Nature* 282:253–256.

Deeming, J. E. (1995), Development of a fire danger rating system for East-Kalimantan, IFFM short term report, Document No. 08, Final report, GTZ, Eschborn.

Dozier, J. (1981), A method for satellite identification of surface temperature fields on sub-pixel resolution. *Remote Sens. Environ.* 11:221–229.

Dwyer, E., Grégoire, J.-M., and Malingreau, J.-P. (1998), A global analysis of vegetation fires using satellite images: spatial and temporal dynamics. *Ambio* 27(3):175–181.

Fang, M., and Huang, W. H. (1998), Tracking the Indonesian Forest Fire using NOAA-AVHRR images. *Int. J. Remote Sens.* 19(3):387–390.

Frederiksen, P., Langaas, S., and Mbaye, M. (1990), NOAA-AVHRR and GIS-based monitoring of fire activity in Senegal—a provisional methodology and potential applications. In *Fire in the Tropical Biota. Ecosystems Process and Global Challenge* (J. G. Goldammer, Ed.) Ecological Studies 84, Springer-Verlag, Berlin, Heidelberg, New York, pp. 400–417.

French, N. H., Kasischke, E. S., Bourgeau-Chavez, L. L., and Berry, D. (1995), Mapping the location of wildfires in Alaskan boreal forest using AVHRR Imagery. *Int. J. Wildland Fire* 5(12):55–61.

French, N. H., Kasischke, E. S., Bourgeau-Chavez, L. L., and Harrel, P. A. (1996), Sensitivity of ERS-1 SAR to variations in soil water in fire disturbed boreal forest ecosystems. *Int. J. Remote Sens.* 17:3037–3053.

Fuller, D. O., and Fulk, M. (1998), An assessment of fire distribution and impacts during 1997 in Kalimantan, Indonesia using satellite remote sensing and geographic information systems, a final report The World Wide Fund for Nature, Indonesia Program, Jakarta, Indonesia.

Grégoire, J.-M. (1996), Use of AVHRR data for the study of vegetation fires in Africa: fire management perspectives. In *Advances in the Use of NOAA AVHRR Data for Land Applications* (G. D'Souza, Eds.), ECSC, EEC, EAEC, Brussels and Luxembourg, pp. 311–355.

Grégoire, J.-M., Barbosa, P., Dwyer, E., et al. (1996), Vegetation fire research at the Monitoring Tropical Vegetation Unit: product availability—June 1996, Fire in the global resource and environmental monitoring, Eur. 16433, Joint Research Center, European Commission, Ispra, Italy.

Hao, W. H., Lui, M.-H., and Crutzen, P. J. (1990), Estimates of annual and regional releases of CO_2 and other trace to the atmosphere from fires in the tropics. Based on the FAO statistics for the period 1975–1980. In *Fire in the Tropical Biota, Ecosystems Process and Global Challenge*. (J. G. Goldammer, Ed.), Ecological Studies 84, Springer-Verlag, Berlin, Heidelberg, New York, pp. 371–383.

Herisoa, R., Frouin, R., Iacobellis, S. F., and Somerville, R. C. J. (1995), Methodology for estimating burned area from AVHRR reflectance data. *Remote Sens. Environ.* 54: 273–289.

Hoffmann, A. A., and Christy, L. (1998), Daily fire observation from space in East-Kalimantan. *Int. For. Fire News* 19 (Oct.):20–22.

Kaufmann, Y. J., Setzer, A., Justice, C., Tucker, C. J., Perreira, M. G., and Fung, I. (1990a), Remote sensing of biomass burning in the tropics. In *Fire in the Tropical Biota, Ecosys-*

tems Process and Global Challenge (J. G. Goldammer, Ed.). Ecological Studies 84, Springer-Verlag, Berlin, Heidelberg, New York, pp. 371–399.

Kaufmann, Y., Tucker, C. J., and Fung, I. (1990b), Remote sensing of biomass burning in the tropics. *J. Geophys. Res.* 95:9927–9939.

Kennedy, P. J., Belward, A. S., and Grégoire, J.-M. (1994), An improved approach to fire monitoring in West Africa using AVHRR data. *Int. J. Remote Sens.* 15:2235–2255.

Kuntz, S., Streck C., and Siegert, F. (1996), Multitemporal evaluation of ERS-SAR data for monitoring deforestation in tropical rain forests. In *Proceedings of the 2 ERS-1/2 Applications Workshop*, London, ESA SP-383, European Space Agency, Paris, pp. 83–93.

Liew, S. C., Lim, O. K., Kwoh, L. K., and Lim, H. (1998), A study of the 1997 forest fires in South East Asia using SPOT Quicklook mosaics. *International Geoscience and Remote Sensing Symposium*, 6–10 July, Seattle, Center for Remote Imaging, Sensing and Processing, National University of Singapore.

Malingreau, J.-P. (1990), The contribution of remote sensing to the global monitoring of fires in tropical and subtropical ecosystems. In *Fire in the Tropical Biota, Ecosystems Process and Global Challenge* (J. G. Goldammer, Ed.). Ecological Studies 84, Springer-Verlag, Berlin, Heidelberg, New York, pp. 337–370.

Malingreau, J.-P., and Grégoire, J.-M. (1996). Developing a global vegetation fire monitoring system for global change studies: a framework. In *Biomass Burning and Global Change* (J. S. Levine, Ed.), The MIT Press, Cambridge, MA, Vol. 1, pp. 14–24.

Malingreau, J. P., Stephens, G., and Fellows, L. (1985), Remote sensing of forest fires: Kalimantan and North Borneo in 1982–83. *Ambio* 14(6):314–321.

Malingreau, J.-P., Jones, S. H., Dwyer, E., and Pinnock, S. (1996), Regional vegetation fire patterns in Southeast Asia. A satellite-based assessment. *Conference on Transboundary Pollution and the Sustainability of Tropical Forests*, Asean Institute of Forest Management, Ampang Press, Kuala Lumpur, Malaysia, 2–4 December.

Rignot, E., Salas, W. A., and Skole, D. L. (1997), Mapping deforestation and secondary growth in Rondonia, Brazil, using imaging radar and Thematic Mapper data. *Remote Sens. Environ.* 59:167–179.

Schindele, W., Thoma, W., and Panzer, K. (1989), The forest fire 1982/83 in East Kalimantan. Part I. GTZ-PN: 38 3021:3–11 GTZ, Eschborn, Germany.

Siegert, F., and Kuntz, S. (1999), Land use classification using multitemporal ERS-SAR Data. *Int. J. Remote Sens.* 20(4): 2835–2853.

Siegert, F. and Rücker, G. (1999), Evaluation of the 1998 forest fires in East-Kalimantan (Indonesia) using multitemporal ERS-2 SAR images. *Earth Obs. Quart.* 61:7–12.

Siegert, F., and Rücker, G. (2000), Use of multitemporal ERS-2 SAR images for identification of burned scars in South-East Asian tropical rainforest. *Int. J. Remote Sens.*, in press.

Schweithelm, J. (1998), The fire this time, An overview of Indonesia's forest fires in 1997/98, World Wide Fund for Nature Discussion paper, WWF Indonesia Programme, Jakarta.

Ulaby, F. T., Moore, R. K., and Fung, A. K. (1986), The backscattering behaviour of random surfaces. In *Microwave Remote Sensing: Active and Passive, Vol. III: From Theory to Applications*, Artech House, Dedham, pp. 1811–1830.

Wooster, M. J., Ceccato, P., and Flasse, S. P. (1998), Indonesian fires observed using AVHRR. *Int. J. Remote Sens.* 19:383–386.

Wannamaker, B. (1996), Sea scan STARS user manual, Sea Scan Oceanographic and Remote Sensing Consultants, Toronto, Canada, unpublished.